*materials*

MDPI

*Article*

# Mechanical Properties and Equilibrium Swelling Characteristics of Some Polymer Composites Based on Ethylene Propylene Diene Terpolymer (EPDM) Reinforced with Hemp Fibers

**Maria Daniela Stelescu [1], Anton Airinei [2,*], Alexandra Bargan [2], Nicusor Fifere [2], Mihai Georgescu [1], Maria Sonmez [1], Mihaela Nituica [1], Laurentia Alexandrescu [1] and Adriana Stefan [3]**

[1] National Research and Development Institute for Textile and Leather, Leather and Footwear Institute, 93 Ion Minulescu Street, 031215 Bucharest, Romania
[2] Petru Poni Institute of Macromolecular Chemistry, 41A Grigore Ghica Voda Alley, 700487 Iasi, Romania
[3] National Institute of Aerospace Research "Elie Carafoli", 220 Iuliu Maniu Blv., 061126 Bucharest, Romania
* Correspondence: airineia@icmpp.ro

**Abstract:** EPDM/hemp fiber composites with fiber loading of 0–20 phr were prepared by the blending technique on a laboratory electrically heated roller mill. Test specimens were obtained by vulcanization using a laboratory hydraulic press. The elastomer crosslinking and the chemical modification of the hemp fiber surface were achieved by a radical reaction mechanism initiated by di(tert-butylperoxyisopropyl)benzene. The influence of the fiber loading on the mechanical properties, gel fraction, swelling ratio and crosslink degree was investigated. The gel fraction, crosslink density and rubber–hemp fiber interaction were evaluated based on equilibrium solvent-swelling measurements using the Flory–Rehner relation and Kraus and Lorenz–Park equations. The morphology of the EPDM/hemp fiber composites was analyzed by scanning electron microscopy. The water absorption increases as the hemp fiber loading increases.

**Keywords:** EPDM rubber; hemp fiber; crosslink density; mechanical properties; water uptake; reinforcement



**Citation:** Stelescu, M.D.; Airinei, A.; Bargan, A.; Fifere, N.; Georgescu, M.; Sonmez, M.; Nituica, M.; Alexandrescu, L.; Stefan, A. Mechanical Properties and Equilibrium Swelling Characteristics of Some Polymer Composites Based on Ethylene Propylene Diene Terpolymer (EPDM) Reinforced with Hemp Fibers. *Materials* **2022**, *15*, 6838. https://doi.org/10.3390/ma15196838

Academic Editor: Carola Esposito Corcione

Received: 17 August 2022
Accepted: 27 September 2022
Published: 1 October 2022



## 1. Introduction

Reinforced polymer composites with cellulosic natural fibers have gained increasing importance in recent years, both in the scientific community and in industry. Natural cellulosic fibers have become promising materials to obtain reinforcing agents that can replace inorganic fillers, such as carbon black, silica, etc. Natural fibers offer some advantages, such as easy availability, lower cost, renewable nature, production with less environmental pollution and low health hazards. In addition, the use of natural fibers as a replacement to inorganic fillers is determined by their good mechanical properties, non-toxic nature, non-abrasive behavior on processing equipment and low emission level during incineration at their end of life. Despite these attractive properties, natural fibers used as reinforcing agents have a few disadvantages, such as high level of moisture absorption, lower thermal stability and hydrophilic character, which can lead to incompatibility with hydrophobic polymer matrices. The characteristics of natural fibers depend on climatic conditions, plant species, the harvesting period, the processing conditions, etc. [1–6].

Natural fibers are mainly composed of cellulose, lignin, hemicelluloses, pectin, waxes, etc. The chemical composition depends on the type of natural fiber and varies even if they belong to the same family [5,7–9]. These compounds, due to their a high content of hydroxyl and polar groups, impart a hydrophilic character to cellulosic natural fibers, leading to poor interfacial interactions with hydrophobic polymer materials. In this way, in order to obtain polymer composites with superior properties, the surface of natural fibers is modified by

chemical or physical methods to improve their adherence to the polymer matrix. Chemical treatments such as mercerization, acetylation, maleated coupling, physical treatments (cold plasma treatment, thermal treatment, corona dischargers) or enzymatic procedures were applied to modify the surface of the natural fibers by removing some surface OH-groups [10–15]. These methods that treat the surface of natural fibers represent distinct stages in the technological flux to obtain polymer composites reinforced with natural fibers, consequently increasing the working time and the final cost of the composites.

EPDM (ethylene propylene diene terpolymer) rubber has attracted tremendous interest in the industry due to its high resistance to aging, heat, polar solvents and other chemicals, as well as owing to its excellent electrical characteristics and mechanical properties. In addition, EPDM rubber can be processed without difficulties, accepting high levels of fibers, reinforcing agents and plasticizers. The formulation and manufacture of the novel polymer composites based on EPDM and hemp fibers, respecting the requirements of the circular economy, contribute to the diversification of the field of eco-polymer materials and to the improvement of the existing technologies. Due to the advantages of polymer composites reinforced with vegetal fibers, these materials can be used in various applications, such as automotive, aerospace, buildings and construction industries [16–22], contributing to the reduction in the components' weight in the final product, improving the damping characteristics to shocks and vibrations of the material [23,24], as well as its thermal and phonic isolation properties [23–25]. Furthermore, these composites assure easier processing, higher resistance to extreme temperature variations, and have a low impact on the environment [16–19].

Hemp (*Cannabis sativa* L.) is an annual plant with a long cultivation history. This plant demonstrates rapid growth, with lower labor requirements and small fertilizer and pesticide dependence. In suitable conditions, the plants can reach 300–1500 mm [4,7–9].

In the present work, composites based on EPDM and hemp fibers were obtained. The modification of the hemp fiber surface was performed by a radical reaction mechanism initiated by peroxide, at high temperature during the crosslinking process of the elastomer. The effect of the reinforcing agent loading (hemp fibers) on the physico-mechanical properties, crosslinking density, gel fraction and morphology of the composites was investigated. Moreover, the reaction mechanisms that occur during the crosslinking and grafting process of the EPDM/hemp fiber composites, as well as the characterization of these composites, were discussed.

## 2. Experimental Section

### *2.1. Materials*

Ethylene propylene diene terpolymer (EPDM) Nordel 4760 from Dow Chemical Company was used as the polymer matrix. This polymer contains 70 wt % ethylene and 4.9 wt % ethylenenorbornene (ENB), with a Mooney viscosity of 70 $ML_{1+4}$ at 120 °C, density of 0.88 g/cm$^3$ and crystallinity degree of 10%. As a lubricating agent, polyethylene glycol (PEG) with medium molecular weight was added. PEG 4000 was supplied by Advance Petrochemicals LTD, with a density of 1.128 g/cm$^3$, and melting point in the range of 4–8 °C. It is a flaky solid, easy to process and add to other materials, difficult to precipitate, and has good compatibility with rubber. It can greatly increase the plasticity of rubber products, and effectively reduce the power loss in production processes. In addition, PEG 4000 can contribute to the homogeneous dispersion of the hemp fibers in the EPDM matrix [26–28]. A sterically hindered phenolic antioxidant, namely Irganox 1010 (pentaerythritol tetrakis(3-3,5-di-tert-butyl-4-hydroxy)propionate), was added to assure the protection against the thermooxidative degradation and for long-term thermal stabilization. It was bought from BASF Schweiz (melting point of 40 °C, active ingredient of 98% and density of 1.15 g/cm$^3$). The reinforcement of the rubber composites was made using ground hemp fiber threads, with a length of 2.5 mm. Perkadox 14-40B di(tert-butylperoxyisopropyl)benzene, used as a vulcanizing agent, was obtained from Akzo Nobel Chemicals (density of 1.60 g/cm$^3$, active oxygen content of 3.8%, peroxide content of 40%). In order to determine the crosslink

density and the gel fraction, n-hexane (Merck KGaA, Darmstadt, Germany) was utilized as a solvent.

### 2.2. Preparation of EPDM/Hemp Fiber Composites

EPDM-based composites were obtained by the blending method, on a laboratory electrically heated roller mill, equipped with a cooling system (Brabender GmbH&Co KG, Duisburg, Germany) (Scheme 1). The working conditions included friction 1:1.1, and temperature of 60–90 °C. The nomenclature of the different samples and the EPDM composite formulations are listed in Table 1. First, EPDM was introduced into the roller mill (2 min), then the antioxidant (Irganox1010) and PEG 4000 were incorporated and mixed for another 2 min. When a homogeneous mixture was obtained, predetermined amounts of ground hemp fibers (0, 5, 10, 15 and 20 phr, respectively) were added and further mixed for 4 min. The sample EP0, without hemp fibers, was considered as the control sample. At the end, the vulcanizing agent was added (1 min) and the mixture was homogenized for 5 min and then removed from the roll in the form of a sheet about 2 mm thick. The vulcanization was carried out using a laboratory hydraulic press (Fortune Press, model TP/600, Fontijine Grotness Vlaardingen, The Netherlands) at 160 °C, pressing force of 300 kN and vulcanization time of 20 min. Subsequently, the specimens were cooled to 45 °C under the pressure force of 300 kN and cooling time of 10 min.

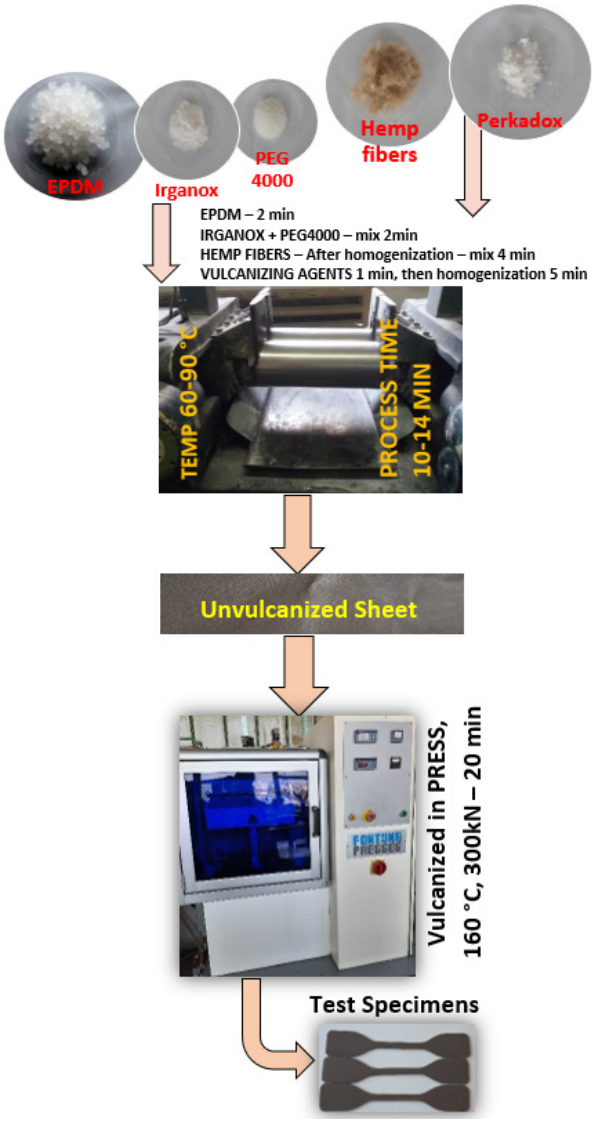


**Scheme 1.** Schematic illustration for the preparation of the EPDM-based composites.

**Table 1.** Composite formulations [a].

| Ingredients | Sample | | | | |
|---|---|---|---|---|---|
| | **$EP_0$** | **EP5Ca** | **EP10Ca** | **EP15Ca** | **EP20Ca** |
| Polymer matrix, EPDM | 100 | 100 | 100 | 100 | 100 |
| reinforcing agent, hemp | 0 | 5 | 10 | 15 | 20 |
| Lubricating agent, PEG 4000 | 3 | 3 | 3 | 3 | 3 |
| Antioxidant, Irganox 1010 | 1 | 1 | 1 | 1 | 1 |
| Vulcanizing agent, Perkadox 14-40B | 8 | 8 | 8 | 8 | 8 |

[a] Parts to 100 parts rubber (phr).

### *2.3. Measurements*

The hardness (in Shore A) of EPDM-based composites was determined on a hardness tester according to ISO 48-4 and ASTM D2240, using samples with the thickness of 6 mm. The elasticity was measured on a Schob test instrument on 6 mm thick samples according to ISO 4662 and ASTM D78121-05. The tensile strength, elongation at break and modulus at 100% were measured using dumb-bell shaped specimens according to ISO 37 and ASTM D41 on a Schopper strength tester at a testing speed of 500 mm/min. Equilibrium solvent swelling measurements were taken in hexane at 23–25 °C. The samples were cut in the form of discs with the diameter of 20 mm and thickness of 2 mm. For each sample, three discs were used. The samples were dried at 100 °C for 60 min, then weighed ($m_i$) and immersed in dark color bottles with lids, in which hexane was introduced. The immersion time was 168 h to attain the equilibrium. After immersion, the samples were reweighed ($m_s$). Furthermore, the samples were dried at room temperature for 6 days and then at 70 °C for 3 h to remove solvent traces, and finally, the samples were weighed again ($m_d$). Gel fraction was calculated according to Equation (1) [26,29].

$$Gel\ fraction(\%) = \frac{m_d}{m_i} \times 100 \quad (1)$$

The crosslink density, ν, was determined using the Flory–Rehner equation for tetra-functional networks, Equation (2) [30].

$$\nu_{cross}\left(\frac{mol}{g}\right) = \frac{1}{2M_c} = -\frac{ln(1-V_r) + V_r + \chi_{12}V_r^2}{2V_s\left(\sqrt[3]{V_r} - \frac{V_r}{2}\right)} \quad (2)$$

where $M_c$ is the average molecular weight of the rubber between the crosslinks, $V_r$ is the volumetric fraction of rubber at swelling equilibrium, $\chi_{12}$ describes the Flory–Higgins polymer–solvent interaction parameter and $V_s$ is the solvent molar volume (130.77 $cm^3/mol$ for n-hexane).

The volume fraction of rubber in the swollen sample $V_{ro}$ for rubber composites that do not contain reinforcing agent can be estimated by the Equation (3) [31,32].

$$V_{r0} = \frac{Volume\ of\ rubber}{(Volume\ of\ rubber) + (Volume\ of\ solvent)} = \frac{\frac{m_d}{\rho_r}}{\frac{m_d}{\rho_r} + \frac{m_s - m_d}{\rho_s}} \quad (3)$$

where $\rho_s$ represents the solvent density, $\rho_r$ is rubber sample density and $(m_s - m_d)$ is the weight of solvent in the swollen rubber. The density of the elastomer samples was measured according to ISO 2781.

For the EPDM composites containing reinforcing agent, in the expression of $V_{ro}$, the fractions of insoluble compounds must be eliminated and the relation for $V_{rf}$ becomes Equation (4) [10,33–35].

$$V_{rf} = \frac{\frac{m_d - \varphi_h * m_i}{\rho_r}}{\frac{m_d - \varphi_h * m_i}{\rho_r} + \frac{m_s - m_d}{\rho_s}} \quad (4)$$

where $\varphi_h$ denotes the volume fraction of hemp fibers, evaluated from Equation (5), which is as follows:

$$\varphi_h = \frac{\frac{m_h}{\rho_h}}{\frac{m_h}{\rho_h} + \frac{m_r}{\rho_r}} \quad (5)$$

where $m_h$ is the weight of hemp fibers from the sample, $\rho_h$ is the hemp fiber density, $m_r$ is the weight of EPDM rubber and $\rho_r$ is its density.

The Flory–Higgins polymer–solvent interaction parameter $\chi_{12}$ is a measure of the interaction energy of solvent molecules with rubber, and it can be estimated using Equation (6) [36–39].

$$\chi_{12} = \beta + \frac{V_s}{RT}(\sigma_r - \sigma_s)^2 \quad (6)$$

where $\beta$ represents the lattice constant for the polymer–solvent system ($\beta$ = 0.34), $R$ is the universal constant of gases, $T$ is the absolute temperature, $\sigma_r$ and $\sigma_s$ describe the solubility parameter of the rubber sample and solvent, respectively [40].

The dynamic water vapor sorption was measured with an IGAsorp dynamic sorption analyzer (Hiden Analytical, Warrington, PA, USA), equipped with an ultrasensitive microbalance, which allows one to observe the modifications in the sample mass as a function of the relative humidity (RH). Before sorption experiments, each sample was dried in nitrogen flow (250 mL/min), until their weight reached the equilibrium at a relative humidity of <1%. The determinations were performed at 25 °C in a RH range of 0–90%, by humidity steps of 10%, with each step consisting of a pre-established equilibrium time between 40 and 60 min.

Fourier transform infrared (FTIR) spectra of all the samples were achieved on a Nicolet IS50 FT-IR spectrometer (ThermoFisher Scientific, Bremen, Germany) in the wavenumber range of 4000–400 $cm^{-1}$, using attenuated total reflection (ATR).

The morphology of the EPDM-based composites was analyzed using a Quanta 250 scanning electron microscope (FEI, Brno, the Czech Republic) on square shaped samples of 10 × 10 mm, with a magnification between 100 and 10.000. For the morphostructural measurements, a conductive layer was deposited on the sample surface.

## 3. Results and Discussion

### *3.1. Reaction Mechanism*

The crosslinking of EPDM/hemp fibers, as well as the chemical modification of the hemp fibers, was carried out at 160 °C using Perkadox 14-40B as a crosslinking agent. The crosslinking process takes place in several stages, which are as follows. The initiation stage of the crosslinking reaction occurs in two successive steps (Scheme 2). In the first step, the crosslinking agent (Perkadox 14-40B) decomposes at 135–160 °C and the free radicals RO ·or R are formed. These radicals are active species and they will react with both EPDM elastomer and the cellulose, the main component of the vegetal fiber. In the second step, due to the formed free radicals, hydrogen atom abstraction can occur from the EPDM polymer chains and from polymeric components of the hemp fibers. In the EPDM matrix, the abstraction of hydrogen atoms will occur probably at the $–CH_2—$and = CH- units from the polymer main chain and at the allylic positions $C_3$ and $C_9$ of the diene unit (Scheme 2), forming alkyl EPDM and allyl macroradicals [9,41–43]. In addition, at the interface between the elastomer matrix and the polymeric components of the hemp fibers, some reactions between the formed radicals and the polymeric components of hemp fibers can occur. It is well-known that the composition of the hemp fibers includes cellulose (70–74%), hemicellulose (15–20%), lignin (3.5–5.7%), pectin (0.8%) and waxes (1.2–6.2%), depending on the type of the natural fiber, soil nature, climate, etc. [7–9]. In the above-mentioned reaction mechanism, only cellulose was taken into consideration, because it is the main compound in the hemp structure. The reactivity of cellulose is determined by the presence of the three equatorially positioned OH groups in the anhydroglucopyranose

moieties, one primary and two secondary groups [44,45]. In this way, it can be considered that the hydrogen atoms' abstraction can occur from these positions.

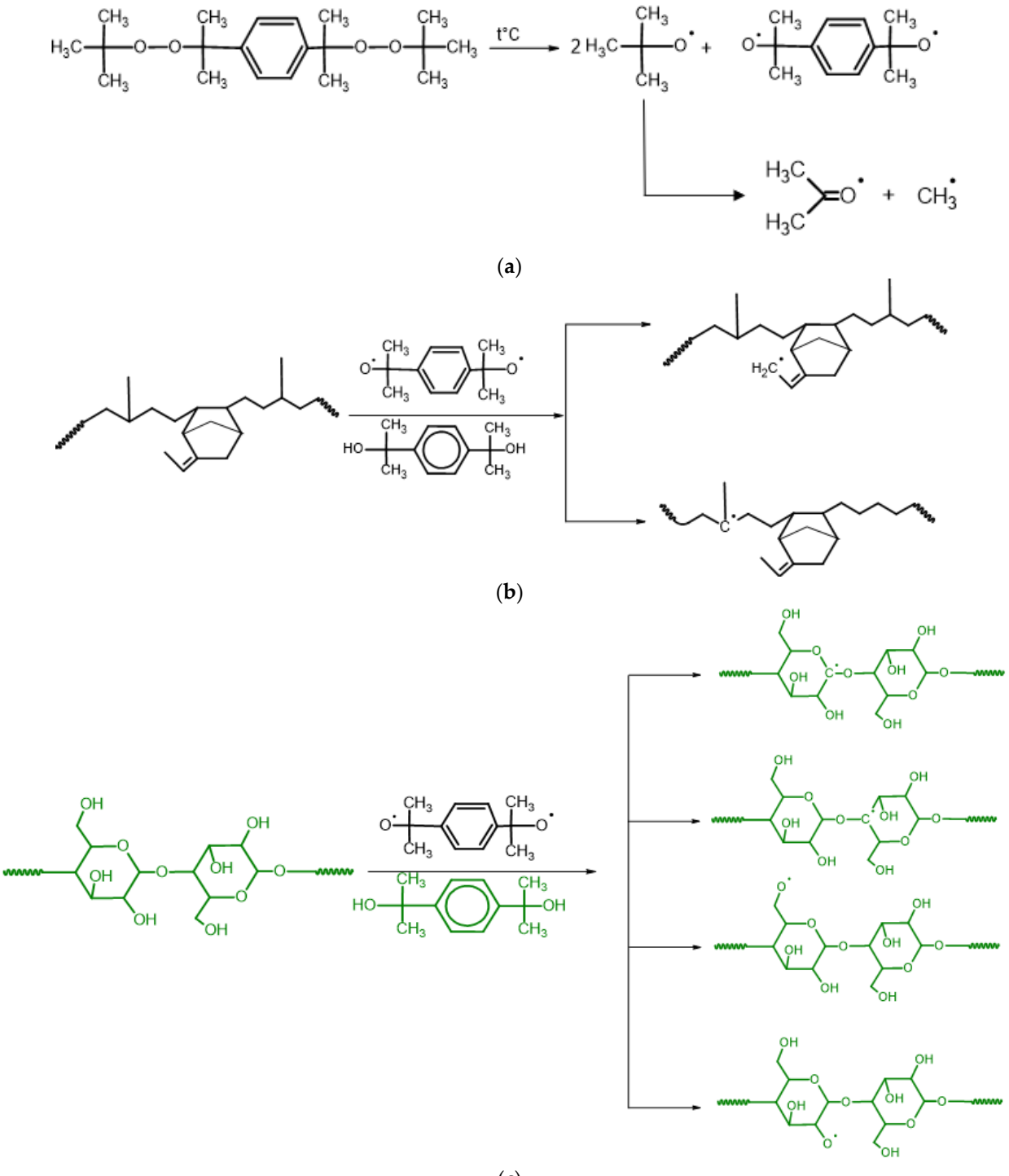


**Scheme 2.** Proposed mechanism for peroxide crosslinking and grafting of EPDM/hemp composites: the initial step of (**a**) decomposition of the peroxide into radicals, (**b**) abstract hydrogen atoms from the EPDM backbone, (**c**) abstract hydrogen atoms from the cellulose backbone.

In the second stage, by the addition reaction between the formed stable macroradicals and the polymeric compounds from the system, the appearance of the crosslinking was detected, with the formation of some macroradicals of higher molecular weight (Scheme 3).

In this case, a three-dimensional network (crosslinked EPDM/hemp) and some structures containing EPDM polymer chains and cellulose or other components from the natural fiber can be formed, which will improve the compatibility between the natural fiber and the elastomer matrix.

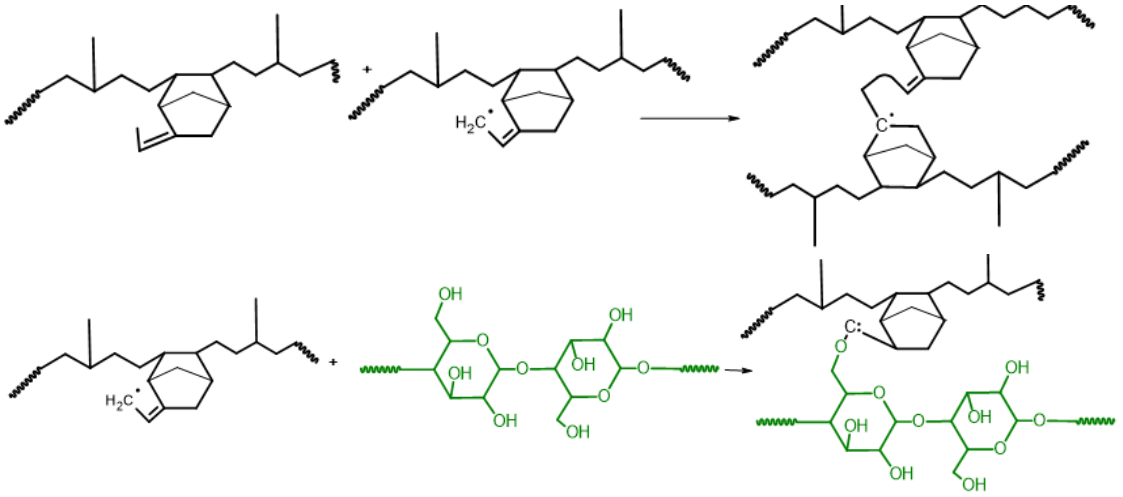

**Scheme 3.** Proposed mechanism for peroxide crosslinking and grafting of EPDM/hemp composites. The addition reactions form macroradicals.

In the termination stage, two possibilities exist. In the termination by a combination process, two growing polymer chains react with the mutual decrease in the growth activity. The termination by recombination (alkyl/allyl, allyl/allyl, alkyl/allyl) of two EPDM macroradicals (EPDM) results in a crosslinking reaction (EPDM-EPDM), the reaction of EPDM macroradicals with cellulose macroradicals (cellulose), forming compatibilizing agents (EPDM-Cellulose), or with peroxide radicals, resulting in a crosslinking inactive reaction (Scheme 4).

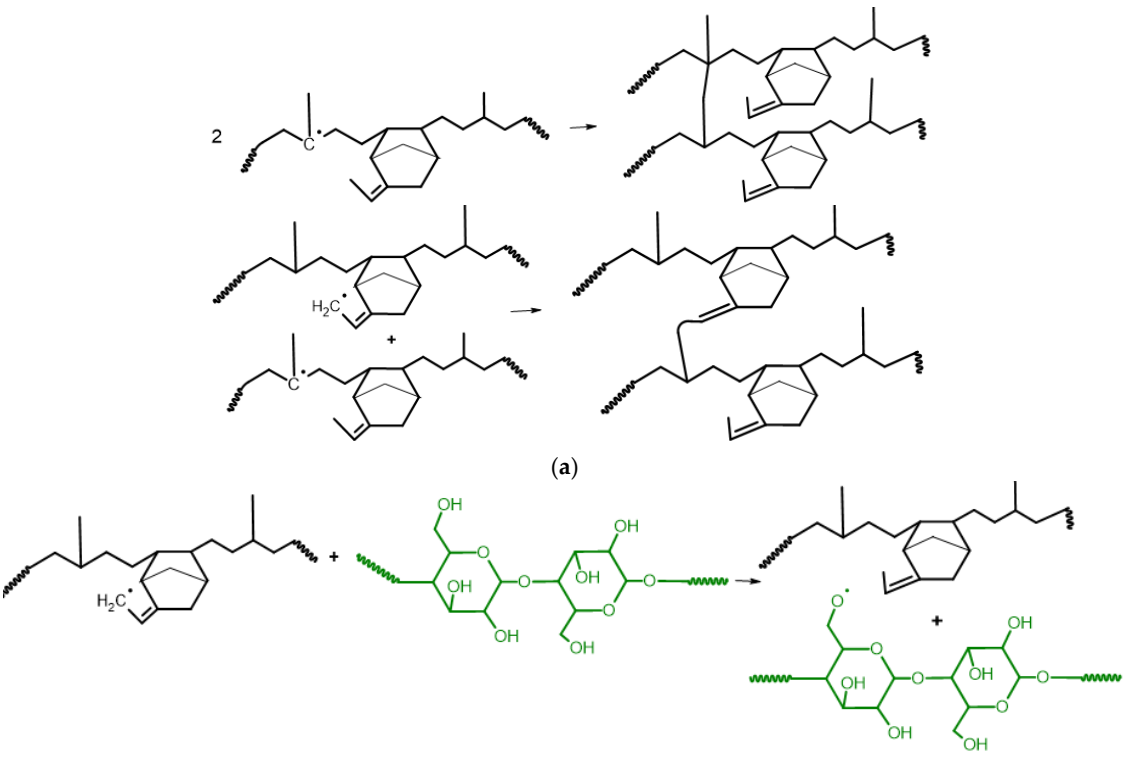

**Scheme 4.** *Cont.*

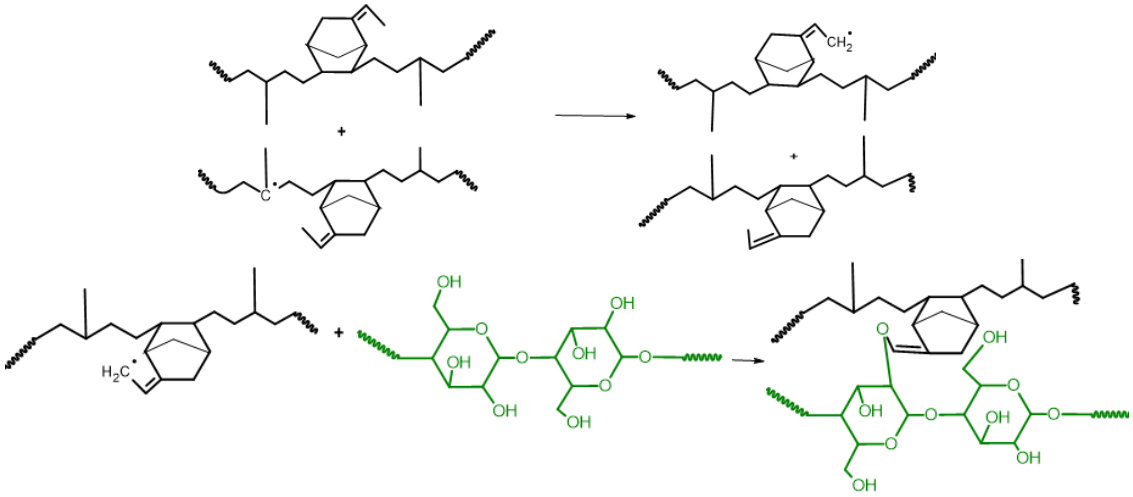

(**b**)

**Scheme 4.** Proposed mechanism for peroxide crosslinking and grafting of EPDM/hemp composites: (**a**) the termination by recombination; (**b**) hydrogen transfer reactions.

In the hydrogen transfer reactions, a growing polymer chain is deactivated by transferring its growth activity to a previously inactive species. The hydrogen transfer reactions can take place from the ENB allylic positions C3 and C9 to radicals formed earlier in the peroxide curing of EPDM, but without the unsaturation being consumed. At the same time, some scission reactions of the polymer chain can occur simultaneously. The number of these reactions increases as the content of propylene units increases in EPDM rubber [46]. Because the EPDM rubber used here contains a low level of propylene units (25.1%), the number of these reactions will be small and the properties of the vulcanized materials will not be affected.

### *3.2. Mechanical Properties*

The mechanical properties have been described by hardness, elasticity, 100% modulus, tensile strength and elongation at break. The hardness of the EPDM/hemp fiber composites increases as the amount of hemp fiber increases, indicating the reinforcing effect of the hemp fibers in EPDM-based composites (Table 2). The maximum hardness was observed for composites loaded by 20 phr hemp fibers (26%). For the other EPDM composites, an increase in hardness of 8% for the EP5Ca sample, 19% for the EP10Ca sample and 23% for the EP15Ca sample, respectively, was recorded. Higher crosslink density in EPDM composites determines higher values of hardness (Tables 1 and 2).

**Table 2.** Mechanical properties of the EPDM/hemp fiber composites.

| Property | Sample | | | | |
|---|---|---|---|---|---|
| | **EP0** | **EP5Ca** | **EP10Ca** | **EP15Ca** | **EP20Ca** |
| Hardness, °ShA | 62 ± 0.58 | 67 ± 1.00 | 74 ± 1.00 | 76 ± 0.58 | 78 ± 0.58 |
| Elasticity, % | 64 ± 0.57 | 56 ± 0.57 | 50 ± 0.57 | 46 ± 0.57 | 46 ± 0.57 |
| 100% modulus, N/mm$^2$ | 1.1 ± 0.03 | 1.4 ± 0.07 | 1.4 ± 0.01 | 1.4 ± 0.01 | 1.3 ± 0.03 |
| Tensile strength at break, N/mm$^2$ | 1.9 ± 0.12 | 1.8 ± 0.06 | 1.8 ± 0.03 | 1.8 ± 0.03 | 1.7 ± 0.03 |
| Elongation at break, % | 287 ± 6.67 | 200 ± 5.77 | 193 ± 6.67 | 220 ± 1.67 | 200 ± 2.89 |

The elasticity (rebound resilience) shows high values for the sample without hemp fiber and then its values decrease as the content of the hemp fibers increases in EPDM composites (Table 2). The reinforced EPDM composites display a decrease in elasticity of 13% for the EP5Ca sample to 28% for the EP20Ca sample, suggesting that the hemp

fibers introduced in the EPDM matrix determine the decrease in elasticity and the segment mobility, in agreement with the results observed for other reinforcement agents [47,48]. The modulus at 100% elongation increases with increasing hemp fiber loading. Thus, an increase of about 27% was obtained for the EPDM composites, due to the fact that the introduction of the reinforcing agent improves the stiffness of the material [49].

The tensile strength of all the composites was reduced with the increasing level of hemp fibers, as compared to the control sample. The decrease in the tensile strength with 5–11% in EPDM composites can be determined by the decrease in the crystallization degree, due to the fiber reinforcement and the increase in the crosslinking degree. In addition, this decrease may be due to an inhomogeneous distribution of the reinforcing agent in the composites, leading to more sites of stress concentration and the decrease in the polymer chain mobility under mechanical loading [49–52]. Moreover, the values of the elongation at break are high, over 193% compared to the control sample, but the decreasing trend as the hemp fiber content increases was maintained. This decrease may be caused by the restriction of the macromolecular chain movements due to the crosslinking formation [53,54].

### *3.3. Equilibrium Swelling Studies*

The equilibrium swelling experiments were used to determine the gel fraction and the crosslink density, as well as the rubber–reinforcing agent interactions, in EPDM composites. The gel fractions were estimated according to relation (1) and in Figure 1, the gel fraction as a function of hemp fiber loading is shown. As can be observed, high values of the fraction gel were obtained over 97%, and a slight increase of 1.12–1.177% was found as the hemp fiber loading increases, reaching 99% for sample EP20Ca as a result of the increase in the reinforcing degree.

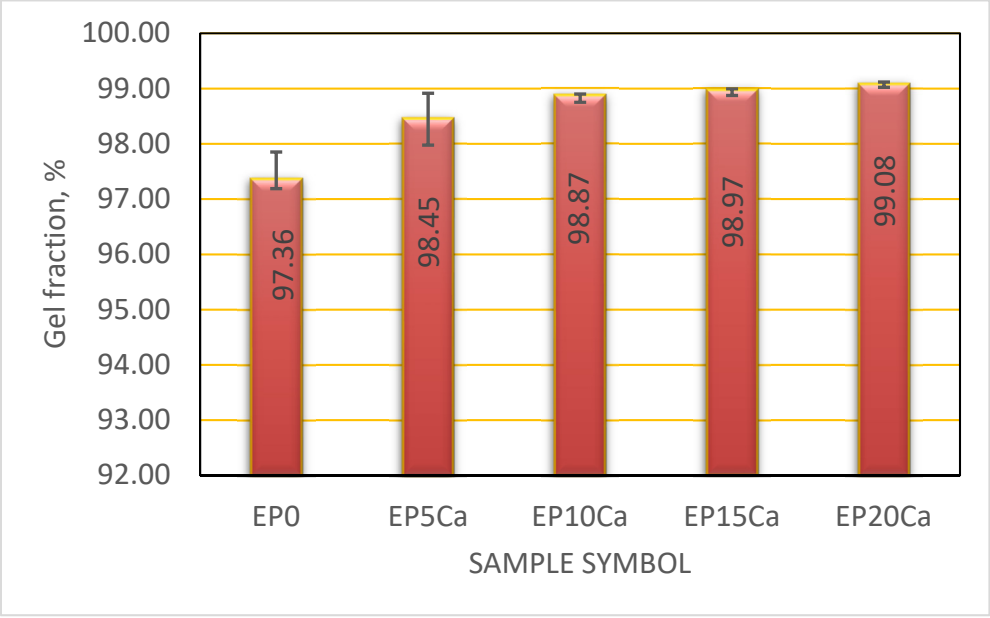


**Figure 1.** Variation in gel fraction as a function of hemp fiber loading.

The crosslink density was determined according to relations (2)–(6), where the value of the Flory–Higgins polymer–solvent interaction parameter, $\chi_{12}$, can be estimated. The solubility parameter of hexane as the solvent is 14.9 $MPa^{1/2}$ [39]. The solubility parameter for EPDM rubber can vary in the range of 15.9–18.6 $MPa^{1/2}$ [39], depending on the elastomer composition. In this way, the EPDM solubility parameter ($\sigma_r$) was evaluated using the

values of molar attraction constants, E, taking into account the structural formula of the polymer and its density, Equation (7) [55,56].

$$\sigma_r = \frac{\rho \sum E}{M} \tag{7}$$

where $\rho$ and $M$ are the density and molecular weight of the polymer repeating unit, respectively. To calculate the parameter $\sigma_r$, we used the structural unit of EPDM with the composition taken from 2.1. The molar attraction constants of the polymer repeating unit (Table 3) were taken from the literature [55,57]. The computed value using relation (7) of the solubility parameter for EPDM rubber Nordel 4760 was found to be 16.5 $MPa^{1/2}$. With this value and using relation (6), the value of the Flory–Higgins polymer–solvent parameter, $\chi_{12}$, was 0.47. The results obtained using the Flory–Rehner equation for the crosslink density are depicted in Figure 2. It can be observed that the crosslink density increases with increasing hemp fiber loading for EPDM composites from 2.64 $\times$ $10^{-4}$ mol/$cm^3$ to 4.03 $\times$ $10^{-4}$ mol/$cm^3$, suggesting the reinforcement of EPDM composites.

**Table 3.** Values of molar attraction constants [55,57].

| Group | E ($MPa^{1/2}$ $cm^3mol^{-1}$) |
|---|---|
| $-CH_3$ | 303 |
| $-CH_2-$ | 269 |
| >CH– | 176 |
| >CH=CH– | 422 |

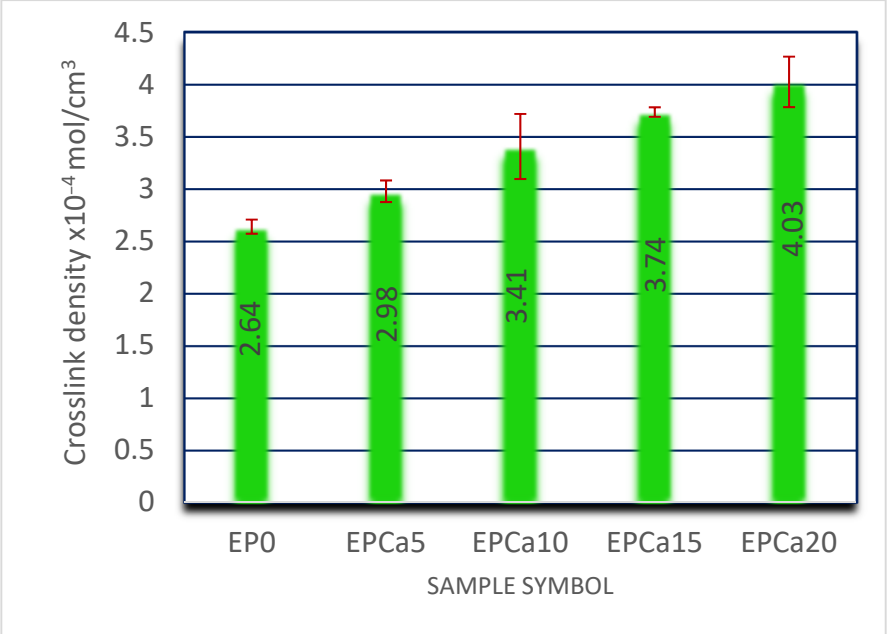


**Figure 2.** Variation in crosslink density with fiber loading for EPDM/hemp fiber composites.

The EPDM matrix reinforcing agent interaction was measured from the equilibrium swelling experiments using the Kraus Equation (8) [58,59].

$$\frac{V_{r0}}{V_{rf}} = 1 - m\left(\frac{\Phi}{1-\Phi}\right) \tag{8}$$

where $V_{ro}$ denotes the volume fraction of the equilibrium swollen rubber without filler (given by Equation (3)), $V_{rf}$ is the volume fraction of the equilibrium swollen rubber with the reinforcing agent (given by Equation (4)), $m$ is the polymer–filler interaction parameter

and Φ is the volume fraction of the fiber. The Kraus plot of the EPDM composite is shown in Figure 3. The value of m can be obtained from the slope of $V_{ro}/V_{rf}$ as a function of $\Phi/(1-\Phi)$. The interaction constant between rubber and filler, C, can be estimated from Equation (9) [32].

$$m = 3C\left(1 - V_{r0}^{1/3}\right) + V_{r0} - 1 \quad (9)$$

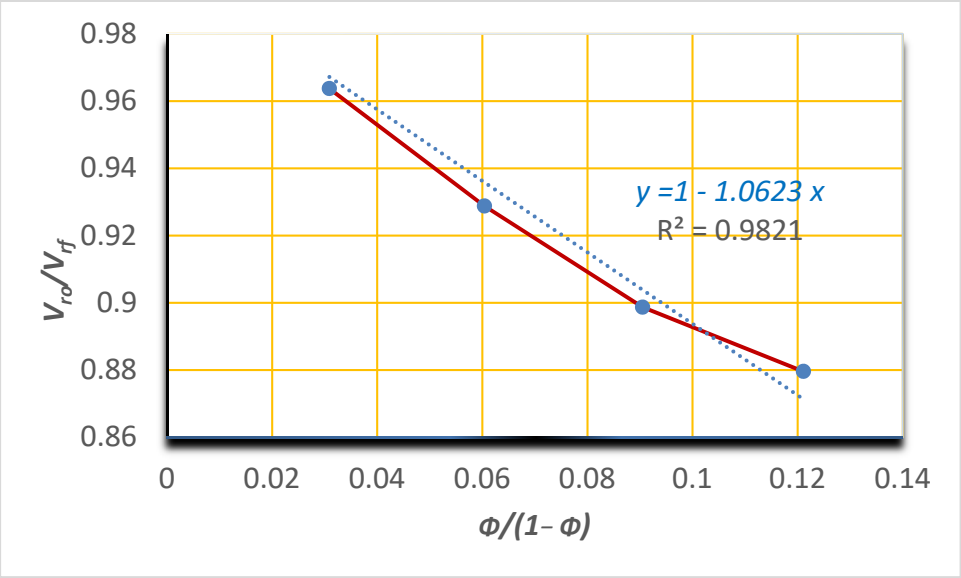


**Figure 3.** Kraus plot for EPDM/hemp fiber composites.

Figure 3 illustrates the decrease in the $V_{ro}/V_{rf}$ ratio as the content of the reinforcing agent increases in the composites, indicating the reinforcement effect of the hemp fibers and improved rubber fiber adhesion. The better interfacial bonds between the reinforcing agent and the polymer matrix hinder the solvent penetration in the matrix and the reinforced vulcanizates present lower values of the ratio $V_{ro}/V_{rf}$ [50,60]. These observations are confirmed by the values of constants m and C. The constants m and C, determined according to Figure 3, have the following values: $m$ = 1.0623 (with a regression coefficient of $R^2$ = 0.9821) and $C$ = 2.1235, respectively. These values suggest a good interaction between the hemp fibers and the elastomer matrix [58,59]. In addition, the negative slope of the Kraus plot indicates the reinforcement effect of the hemp fibers in the composites.

The extent of interactions between EPDM rubber and hemp fibers can be analyzed using the Lorenz–Park Equation (10) [32,61,62].

$$\frac{Q_f}{Q_s} = a\, e^{-z} + b \quad (10)$$

where $z$ is the weight fraction of fiber in the polymer, $a$ and $b$ are constants, $Q_f$ and $Q_s$ represent the amount of solvent absorbed per unit weight of rubber and filled material, respectively, and they are obtained using Equation (11) [32].

$$Q = \frac{m_s - m_d}{m_d} \quad (11)$$

where $m_s$ and $m_d$ are the swollen and dried weight of the compound.

It can be observed from the plot of $Q_f/Q_s$ as a function of $e^{-z}$ (Lorenz–Park plot) that the ratio $Q_f/Q_s$ decreases with increasing hemp fiber loading, suggesting an improvement of the interaction between the EPDM rubber and the hemp fiber. The lowest value of the $Q_f/Q_s$ ratio was obtained for the sample containing 20 phr of the hemp fiber; thus, maximum interaction between the hemp fibers and the EPDM matrix was found for this

loading. The values of constants *a* and *b* are characteristic for each system and they can be obtained from the slope and the intercept of the straight line from Figure 4. It can be observed that the value of parameter *a* is twice the value of parameter *b*, making evident the good interaction between rubber and the reinforcing agent. As can be observed from Figure 4, the combination of the high values of *a* with lower values of *b* leads to strong filler–EPDM rubber interactions [32,63], which is in agreement with the results obtained using the Kraus relation.

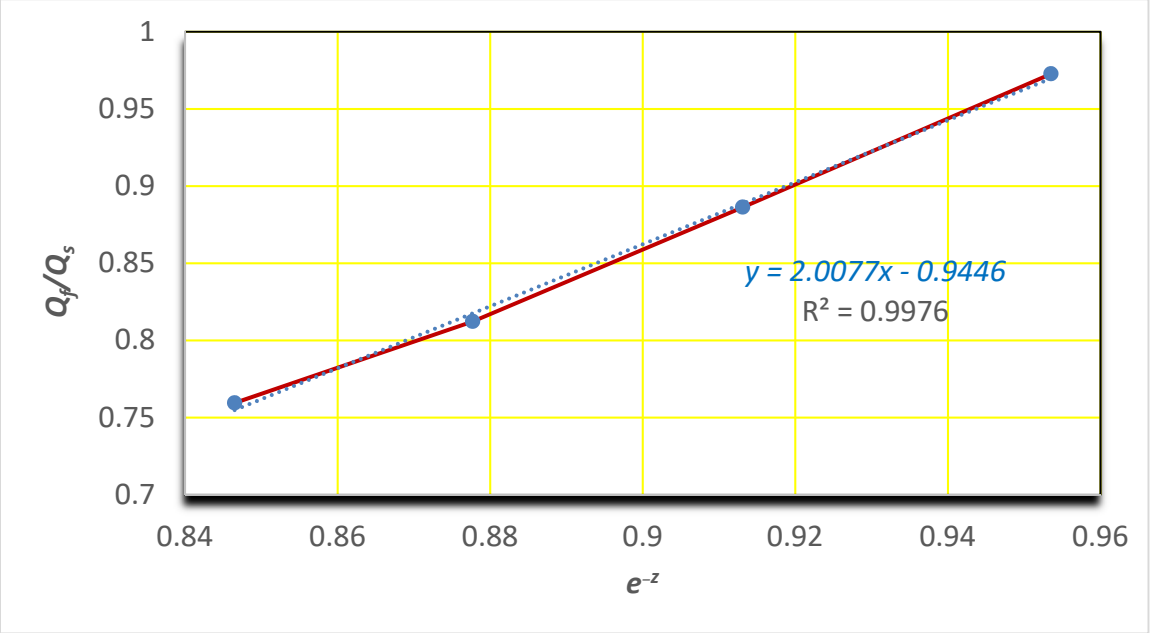


**Figure 4.** Variation in $Q_f/Q_s$ with $e^{-z}$ (Lorenz–Park graph).

### *3.4. FTIR Spectra*

The FTIR spectra of the EPDM/hemp fibers are presented in Figure 5. The IR spectra of the hemp fibers (Figure 5a) showed absorption bands at 2917 and 2850 $cm^{-1}$, due to the CH stretching vibrations of CH and $CH_2$ groups in cellulose and hemicellulose. The absorption band around 3293 $cm^{-1}$ can be assigned to the stretching vibrations of OH groups [64,65]. The absorption bands at 1737 and 1635 $cm^{-1}$ are due to the C=O stretching vibration of carboxylic acid in pectin or ester groups in hemicelluloses and OH bending vibration of bonded water in hemicellulose [64,66]. The absorption band at 1541 $cm^{-1}$ indicates the presence of aromatic rings in lignin. The absorption bands in the range of 1314–1464 $cm^{-1}$ are associated with the deformation vibration of the $CH_2$ and CH groups of cellulose and hemicellulose [67]. The absorption band at 1246 $cm^{-1}$ corresponds to the stretching vibrations of C-O of the acetyl group in hemicellulose and lignin, while the absorption bands at 1102–1158 $cm^{-1}$ are due to asymmetric C-O-C stretching vibrations from the polysaccharide components [66,68]. The FTIR spectra of the crosslinked EPDM rubber (sample EP0) and of EPDM/hemp fiber composites are displayed in Figure 5b. In the FTIR spectrum of the crosslinked EPDM rubber, the strong absorption bands at 2915 and 2850 $cm^{-1}$ are due to the asymmetric and symmetric CH stretching vibrations, the absorption bands at around 1464 and 1377 $cm^{-1}$ are attributed to the $–CH_2$ scissoring vibrations and to CH bending vibration of the $–CH_3$ groups and the absorption band at 720 $cm^{-1}$ corresponds to $–CH_2$ rocking vibrations of the ethylene sequences from the polymer backbone [26,69,70]. The FTIR spectra of the EPDM/hemp composites exhibited absorption bands in the range of 650–700 $cm^{-1}$, assigned to out-of-phase -OH bending in cellulose and hemicellulose and absorption bands located between 1027 and 1158 $cm^{-1}$ due to the CC, C-OH, CH ring and side group vibrations that exist in cellulose, hemicellulose or lignin [64–68].

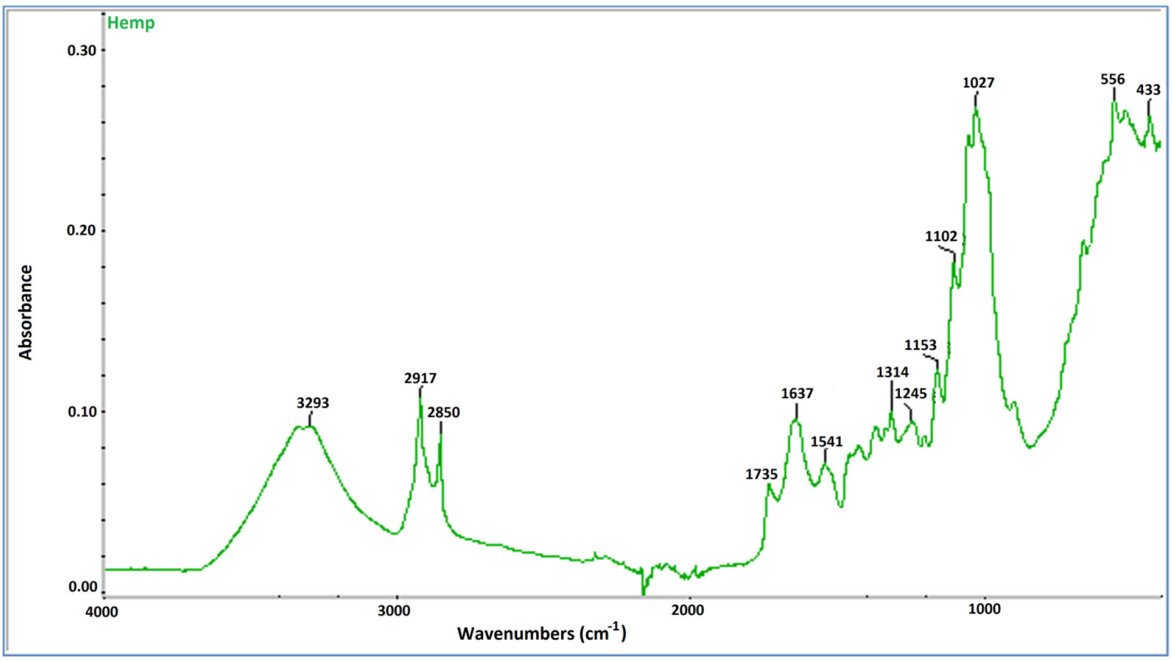


(**a**)

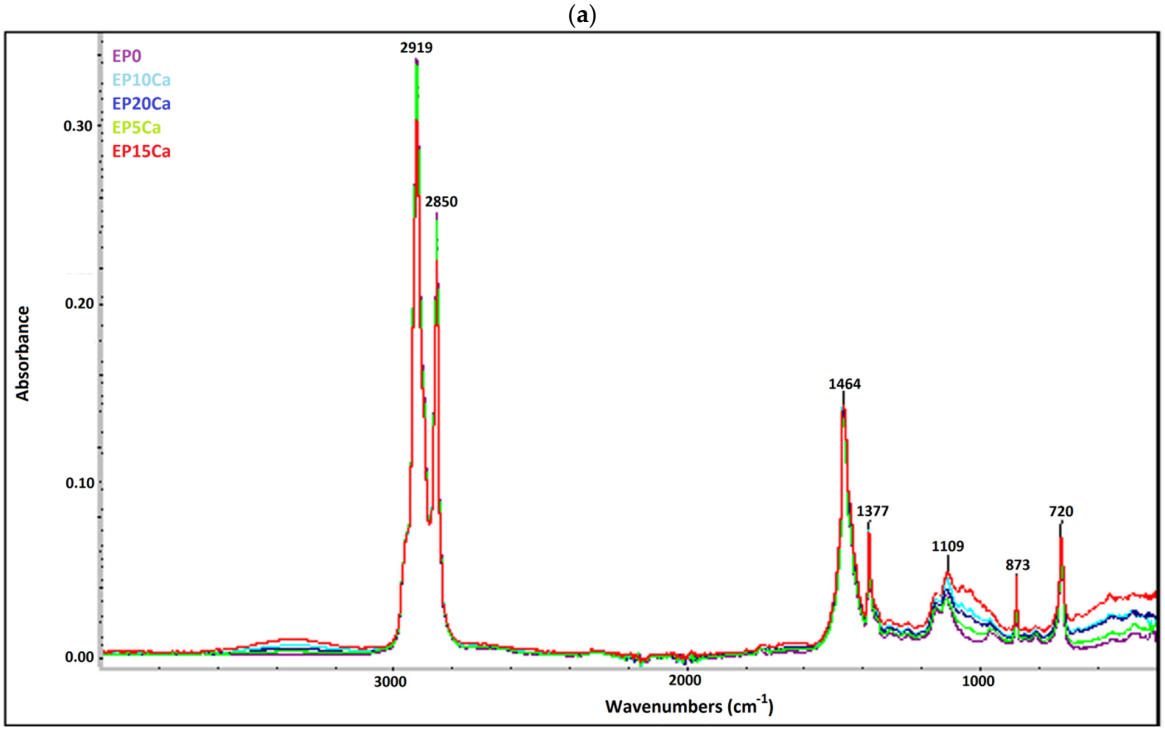


(**b**)

**Figure 5.** FTIR spectra of (**a**) hemp fiber; (**b**) EPDM/hemp fiber composites.

### *3.5. SEM Analysis*

SEM micrographs of the cryogenically fractured surface of the composites were recorded. The surface morphology of the samples EP0 and EP20Ca is shown in Figure 6. From the images, it can be observed that the hemp fibers, together with the other components of the composites, are uniformly dispersed in the elastomer matrix. This quasi-uniform distribution led to good physical and mechanical properties. The fractured surface in the analyzed area has a heterogeneous aspect, both wavy areas and evenly distributed areas are identified and the presence of particles in the polymer mass is highlighted.

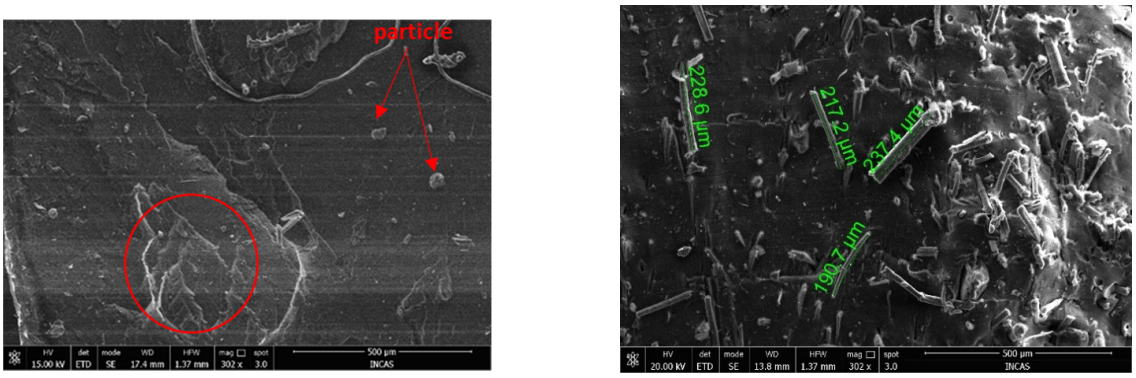


(**a**) EP0 (**b**) EP20Ca

**Figure 6.** SEM micrographs of EPDM/hemp fiber composites (**a**) EP0 and (**b**) EP20Ca.

### *3.6. Water Sorption*

The EPDM/ hemp fiber composites were studied for water absorption behavior and the corresponding sorption/desorption isotherms are displayed in Figure 7. These isotherms can be considered as type IV with H2 pores with an irregular array of sizes and shapes, exemplifying the adsorption behavior of mesoporous materials [71]. It was noticed from Figure 7 that the water absorption increases with the hemp fiber content in the EPDM composites and the highest water uptake was 2.02% for sample EP20Ca. It was observed that, for all the samples, the water absorption rate was slower at the beginning of the process and then the water uptake becomes faster, for RH values over 60%. The water uptake of the EPDM/hemp fiber composites increased because of the hydrophilic nature of the hemp fiber, while the polymer matrix is hydrophobic. The increase in the hemp fiber loading leads to the increase in the free OH groups in composites and to the formation of more hydrogen bonds with water molecules, determining the weight gain of the EPDM/hemp fiber composites [6,9]. In this way, good interfacial adhesion between the elastomer rubber and the hemp fibers enables slight penetration of water molecules into the composite, although the crosslinking prevents the rearrangement of polymer chains during the water absorption process, thus creating resistance to water penetration in the composites [72].

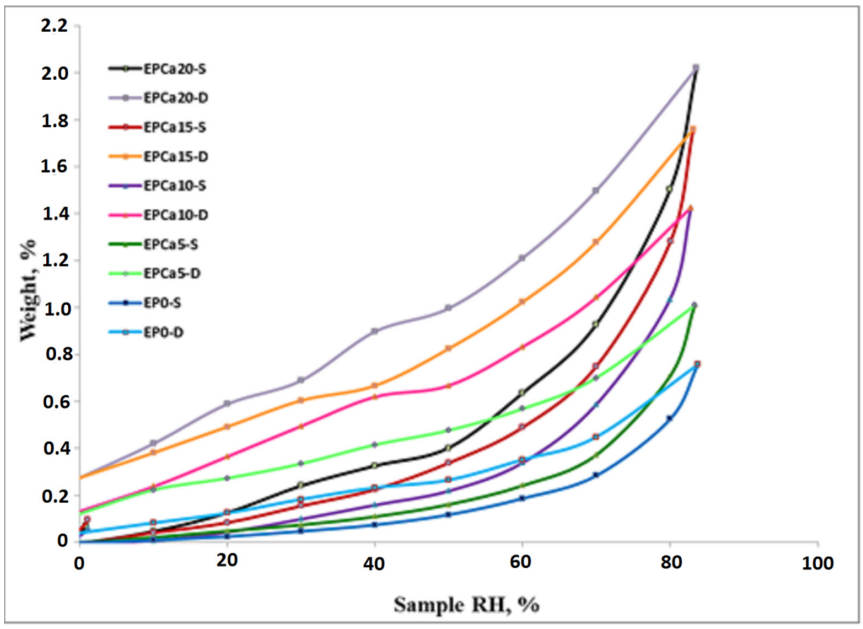


**Figure 7.** Sorption/desorption isotherms of EPDM/hemp fiber composites (S—sorption; D—desorption).

To evaluate the specific surface area, the Brunauer–Emmett–Teller (BET) model was utilized (Equation (12)), by modeling the sorption isotherms registered under dynamic conditions [73].

$$W = \frac{W_m CRH}{(1 - RH)(1 - RH + CRH)} \quad (12)$$

where $W$ represents the sorbed water weight, $RH$ is the relative humidity, $W_m$ is the weight of water forming a monolayer and $C$ is the sorption constant. The values of absorbed water weight are given in Table 4.

**Table 4.** Parameters estimated from sorption/desorption.

| Sample | W (%) | $r_{pm}$ (nm) | BET Data * | |
|---|---|---|---|---|
| | | | Area ($m^2$/g) | Monolayer (g/g) |
| EP0 | 0.7573 | 2.23 | 6.784 | 0.0019 |
| EPCa5 | 1.0091 | 2.67 | 7.561 | 0.0022 |
| EPCa10 | 1.4261 | 1.62 | 17.639 | 0.0050 |
| EPCa15 | 1.7594 | 2.93 | 12.009 | 0.0034 |
| EPCa20 | 2.0199 | 2.09 | 19.329 | 0.0055 |

* Determined based on desorption branch of the isotherm (registered up to a relative humidity of 40%).

The BET model describes the sorption isotherms up to a relative humidity of 40%, relating to the type of the sorption isotherm and the material type. This method can present the isotherms of type II, but also of I, III and IV. The difference between the order of water sorption capacity and the values obtained for the specific surface can be determined by the nature of the functional groups of the polymer from the composite. The average pore size also influences, in a complex way, the sorption capacity of EPDM samples. The BET results are shown in Table 4.

By applying the Barrett, Joyner and Halenda model (BJH), based on the calculation methods for cylindrical pores, the average pore size, $r_{pm}$, was determined using Equations (13) and (14) [74].

$$V_{liq} = \frac{n}{100\rho_a} \quad (13)$$

$$r_{pm} = \frac{2V_{liq}}{A} \quad (14)$$

where $V_{liq}$ is the liquid volume, $n$ is the absorption percentage, $\rho_a$ is the phase density and $A$ represents the specific surface area. The values of the average pore size and of the specific surface area are given in Table 4.

## 4. Conclusions

For the hemp fiber-reinforced EPDM composites, the crosslinking of the EPDM elastomer and the chemical modification of the natural fiber surface were obtained by a radical reaction mechanism initiated by di(tert-butylperoxyisopropyl) benzene at 160 °C. The increase in the hemp fiber content leads to the increase in hardness, gel fraction and crosslink density, indicating the reinforcing effect of hemp fibers. The gel fraction values were over 97% for all composites, with a slight increase for higher hemp fiber loading. The maximum hardness was observed for EPDM composites with higher reinforcing agent levels (15 and 20 phr), namely 76 °ShA and 78 °ShA. The EPDM rubber-reinforcing agent interaction was analyzed using the Kraus relation and the Lorenz–Park equations, and good hemp fiber–rubber interaction was observed, in agreement with SEM analysis. The water absorption of the EPDM/hemp fibers was dependent on the hemp loading. The highest water sorption was 2.02% for the sample with maximum hemp fiber content (20 phr).

**Author Contributions:** Conceptualization and methodology, M.D.S. and A.A.; composite preparation, M.D.S., M.N. and L.A.; investigation, M.D.S., A.A., M.S., A.B., N.F. and A.S.; writing—original draft preparation, M.D.S., A.A. and M.G.; writing—review and editing, A.A. and M.D.S. All authors have read and agreed to the published version of the manuscript.

**Funding:** This research was funded by the Romanian Ministry of Education and Research through Nucleu Project 4R-RCO-MAT PN 19.17.01.03, Contract No. 4N/2019 and PNCDI III C1.2. PFE-CDI 2021, Contract No. 4PFE/2021.

**Institutional Review Board Statement:** Not applicable.

**Informed Consent Statement:** Not applicable.

**Data Availability Statement:** The data presented in this study are available upon request from the corresponding author.

**Conflicts of Interest:** The authors declare no conflict of interest.

## References

1. Lee, B.H.; Kim, H.J.; Yu, W.R. Fabrication of long and discontinuous natural fiber reinforced polypropylene biocomposites and their mechanical properties. *Fibers Polym.* **2009**, *10*, 83–90. [CrossRef]
2. Mohammed, L.; Ansari, M.N.M.; Pua, G.; Jawaid, M.; Islam, M.S. A Review on natural fiber reinforced polymer composite and its applications. *Int. J. Polym. Sci.* **2015**, *2015*, 243947. [CrossRef]
3. Faruk, O.; Bledzki, A.K.; Fink, H.P.; Sain, M. Progress report on natural fiber reinforced composites. *Macromol. Mater. Eng.* **2014**, *299*, 9–26. [CrossRef]
4. Summerscales, J.; Dissanayake, N.P.J.; Virk, A.S.; Hall, W. A review of bast fibres and their composites, Part 1–Fibres as reinforcements. *Composites A* **2010**, *41*, 1329–1335. [CrossRef]
5. Pickering, K.L.; Efendy, M.C.A.; Lee, T.M. A review of recent development in natural fibre composites. *Composites A* **2016**, *83*, 98–112. [CrossRef]
6. Stelescu, M.D.; Manaila, E.; Georgescu, M.; Nituica, M. New materials based on ethylene propylene diene terpolymer and hemp fibres obtained by green reactive processing. *Materials* **2020**, *13*, 2067. [CrossRef]
7. Mochane, M.J.; Mokhena, T.C.; Mokhothu, T.H.; Mtibe, A.; Sadiku, E.R.; Ray, S.S.; Ibrahim, I.D.; Daramola, O.O. Recent progress on natural fiber hybrid composites for advanced applications: A review. *Express Polym. Lett.* **2019**, *13*, 159–198. [CrossRef]
8. Bledzki, A.; Gassan, J. Composites reinforced with cellulose based fibers. *Prog. Polym. Sci.* **1999**, *24*, 221–274. [CrossRef]
9. Dhakal, H.N.; Hang, Z.Z. The use of hemp fibres as reinforcements in composites. In *Biofiber Reinforcements in Composite Materials*; Faruk, O., Sain, M., Eds.; Woodhead Publish.: Cambridge, UK, 2015; pp. 86–103.
10. John, M.J.; Francis, B.; Varughese, K.T.; Thomas, S. Effect of chemical modification on properties of hybrid fiber biocomposites. *Composites A* **2008**, *39*, 352–363. [CrossRef]
11. Nasir, M.; Gupta, A.; Beg, M.D.H.; Chua, G.K.; Kumar, A. Fabrication of medium density fibreboard from enzyme treated rubber wood (*Hevea brasiliensis*) fibre and modified organosolv lignin. *Int. J. Adh. Adh.* **2013**, *44*, 99–104. [CrossRef]
12. George, M.; Mussone, P.G.; Bressler, D.C. Surface and thermal characterization of natural fibres treated with enzymes. *Ind. Crops Prod.* **2014**, *53*, 365–373. [CrossRef]
13. Shalwan, A.; Yousif, B.F. In state of art: Mechanical and tribological behaviour of polymeric composites based on natural fibres. *Mater. Des.* **2013**, *48*, 14–24. [CrossRef]
14. Xie, Y.; Hill, C.A.S.; Xiao, Z.; Militz, H.; Mai, C. Silane coupling agents used for natural fiber/polymer composites: A review. *Composites A* **2010**, *41*, 806–819. [CrossRef]
15. Ray, S.S.; Bousmina, M. Biodegradable polymers and their layered silicate nanocomposites: In greening the 21st century materials world. *Progr. Mater. Sci.* **2005**, *50*, 962–1079.
16. Koronis, G.; Silva, A.; Fontul, M. Green composites: A review of adequate materials for automotive applications. *Composites B Eng.* **2013**, *44*, 120–127. [CrossRef]
17. Loureiro, N.C. Green composites on automotive interior parts: A solution using cellulosic fibers. In *Green Composites for Automotive Applications*; Koronis, G., Arlindo, S., Eds.; Woodhead Publishing: Cambridge, UK, 2019; pp. 81–97.
18. Arockiam, N.J.; Jawaid, M.; Saba, N. Sustainable bio composites for aircraft components. In *Sustainable Composites for Aerospace Applications*; Jawaid, M., Thariq, M., Eds.; Woodhead Publishing: Cambridge, UK, 2018; pp. 109–123.
19. Kopparthy, S.D.S.; Netravali, A.N. Review: Green composites for structural applications. *Compos. Part C Open Access* **2021**, *6*, 100169. [CrossRef]
20. Nurazzi, N.M.; Asyraf, M.R.M.; Khalina, A.; Abdullah, N.; Aisyah, H.A.; Rafiqah, S.A.; Sabaruddin, F.A.; Kamarudin, S.H.; Norrrahim, M.N.F.; Ilyas, R.A.; et al. A review on natural fiber reinforced polymer composite for bullet proof and ballistic applications. *Polymers* **2021**, *13*, 646. [CrossRef]
21. Davoodi, M.M.; Sapuan, S.M.; Ahmad, D.; Aidy, A.; Khalina, A.; Jonoobi, M. Concept selection of car bumper beam with developed hybrid bio-composite material. *Mater. Des.* **2011**, *32*, 4857–4865. [CrossRef]

22. Sassoni, E.; Manzi, S.; Motori, A.; Montecchi, M.; Canti, M. Novel sustainable hemp-based composites for application in the building industry: Physical, thermal and mechanical characterization. *Energy Build.* **2014**, *77*, 219–226. [CrossRef]
23. Tao, Y.; Ren, M.; Zhang, H.; Peijs, T. Recent progress in acoustic materials and noise control strategies—A review. *Appl. Mater. Today* **2021**, *24*, 101141. [CrossRef]
24. Santoni, A.; Bonfiglio, P.; Fausti, P.; Marescotti, C.; Mazzanti, V.; Mollica, F.; Pompoli, F. Improving the sound absorption performance of sustainable thermal insulation materials: Natural hemp fibres. *Appl. Acoust.* **2019**, *150*, 279–289. [CrossRef]
25. Zhu, W.; Chen, S.; Wang, Y.; Zhu, T.; Jiang, Y. Sound absorption behavior of polyurethane foam composites with different ethylene propylene diene monomer particles. *Arch. Acoust.* **2018**, *43*, 403–411.
26. Stelescu, M.D.; Airinei, A.; Manaila, E.; Craciun, G.; Fifere, N.; Varganici, C.; Pamfil, D.; Doroftei, F. Effects of electron beam irradiation on the mechanical, thermal and surface properties of some EPDM/butyl rubber composites. *Polymers* **2018**, *10*, 1206. [CrossRef]
27. Qu, P.; Gao, Y.; Wu, G.F.; Zhang, L.P. Nanocomposites of poly(lactic acid) reinforced with cellulose nanofibrils. *BioResources* **2010**, *5*, 1811–1823.
28. Luo, S.; Cao, J.; Wang, X. Investigation of the interfacial compatibility of PEG and thermally modified wood flour/polypropylene composites using the stress relaxation approach. *BioResources* **2013**, *8*, 2064–2073. [CrossRef]
29. Abdel-Hakim, A.; El-Gamal, A.A.; El-Zayat, M.M.; Sadek, A.M. Effect of novel sunrose based polyfunctional electrical properties of irradiated EPDM. *Rad. Phys. Chem.* **2021**, *189*, 109729. [CrossRef]
30. Flory, P.J.; Rehner, J. Statistical mechanics of cross-linked polymer networks I. Rubberlike elasticity. *J. Chem. Phys.* **1943**, *11*, 512–521. [CrossRef]
31. Bala, P.; Samantaray, B.K.; Srivastava, S.K.; Nando, G.B. Organomodified montmorillonite as filler in natural and synthetic rubber. *J. Appl. Polym. Sci.* **2004**, *92*, 3583–3592. [CrossRef]
32. Hait, S.; De, D.; Ghosh, P.; Chanda, J.; Mukhopadhyay, R.; Dasgupta, S.; Sallat, A.; Al Aiti, M.; Stöckelhuber, K.W.; Wießner, S.; et al. Understanding the coupling effect between lignin and polybutadiene elastomer. *J. Compos. Sci.* **2021**, *5*, 154. [CrossRef]
33. Ellis, B.; Welding, G.N. Estimation, from swelling, of the structural contribution of chemical reactions to the vulcanization of natural rubber. Part I. General method. *Rubber Chem. Technol.* **1964**, *37*, 563–570. [CrossRef]
34. Ellis, B.; Welding, G.N. Estimation, from swelling, of the structural contribution of chemical reactions to the vulcanization of natural rubber. Part II. Estimation of equilibrium degree of swelling. *Rubber Chem. Technol.* **1964**, *37*, 571–575. [CrossRef]
35. Valentın, J.L.; Carretero-Gonzalez, J.; Mora-Barrantes, I.; Chasse, W.; Saalwachter, K. Uncertainties in the determination of cross-link density by equilibrium swelling experiments in natural rubber. *Macromolecules* **2008**, *41*, 4717–4729. [CrossRef]
36. Blanks, R.F.; Prausnitz, J.M. Thermodynamics of polymer solubility in polar and nonpolar systems. *Ind. Eng. Chem. Fundam.* **1964**, *3*, 1–8. [CrossRef]
37. Marzocca, A.J. Evaluation of the polymer–solvent interaction parameter for the system cured styrene butadiene rubber and toluene. *Eur. Polym. J.* **2007**, *43*, 2682–2689. [CrossRef]
38. Marzocca, A.J.; Garraza, A.R.; Mansilla, M. Evaluation of the polymer–solvent interaction parameter for the system cured polybutadiene rubber and toluene. *Polym. Test.* **2010**, *29*, 119–126. [CrossRef]
39. Zielińska, M.; Seyger, R.; Dierkes, W.K.; Bielinski, D.; Noordermeer, J.W.M. Swelling of EPDM rubbers for oil-well applications as influenced by medium composition and temperature Part I. Literature and theoretical background. *Elastomery* **2016**, *20*, 6–12.
40. Simon, D.A.; Barany, T. Effective thermomechanical devulcanization of ground tire rubber with a co-rotating twin-screw extruder. *Polym. Degrad. Stab.* **2021**, *190*, 109626. [CrossRef]
41. van Duin, M. Chemistry of EPDM cross-linking. *Kautsch. Gummi Kunstst.* **2002**, *55*, 150–156.
42. Stelescu, M.D. *High-Performance Thermoplastic Elastomers Based on Ethylene-Propylene Terpolymer Rubber (EPDM) Which Can Be Used in the Footwear Industry*; Performantica Publishing House: Iasi, Romania, 2011.
43. Orza, R.A.; Magusin, P.C.M.M.; Litvinov, V.M.; van Duin, M.; Michels, M.A.J. Mechanism for peroxide cross-linking of EPDM rubber from MAS $^{13}$C NMR spectroscopy. *Macromolecules* **2009**, *42*, 8914–8924. [CrossRef]
44. Granström, M. Cellulose Derivatives: Synthesis, Properties and Applications. Ph.D. Thesis, University of Helsinki, Helsinki, Finland, 2009.
45. Chavan, R.B.; Rathi, S.; Sainaga Jyothi, V.G.S.; Shastri, N.R. Cellulose based polymers in development of amorphous solid dispersions. *Asian J. Pharm. Sci.* **2018**, *14*, 248–264. [CrossRef]
46. Hofmann, W. *Rubber Technology Handbook*; Hanser Publishers: Munnich, Germany, 1989; pp. 93–100.
47. Lee, S.H.; Park, S.Y.; Chung, K.H.; Jang, K.S. Phlogopite-reinforced natural rubber (NR)/ethylene-propylene diene monomer rubber (EPDM) composites with aminosilane compatibilizer. *Polymers* **2021**, *13*, 2318. [CrossRef] [PubMed]
48. Conant, F.S. *Physical testing of vulcanizates, In Rubber Technology*, 3rd ed.; Morton, M., Ed.; Springer Science: Dordrecht, The Netherlands, 1999; pp. 134–178.
49. Nor, N.A.M.; Othman, N. Effect of filler loading on curing characteristic and tensile properties of palygorskite natural rubber nanocomposites. *Procedia Chem.* **2016**, *19*, 351–358. [CrossRef]
50. Wang, J.; Wu, W.; Wang, W.; Zhang, J. Efect of a coupling agent on the properties of hemp-hurd-powder-filled styrene-butadiene rubber. *J. Appl. Polym. Sci.* **2011**, *121*, 681–689. [CrossRef]
51. Stelescu, M.D.; Airinei, A.; Manaila, E.; Craciun, G.; Fifere, N.; Varganici, C. Property correlations for composites based on ethylene propylene diene rubber reinforced with flax fibers. *Polym. Test.* **2017**, *59*, 75–83. [CrossRef]

52. Azahari, N.A.; Othman, N.; Ismail, H. Effect of attapulgite clay on biodegradability and tensile properties of polyvinyl alcohol/corn starch blend film. *Int. J. Polym. Mater.* **2012**, *61*, 1065–1078. [CrossRef]
53. Cristea, M.; Airinei, A.; Ionita, D.; Stelescu, M.D. Relaxation behavior of flax reinforced ethylene-propylene ediene rubber. *High. Perform. Polym.* **2015**, *27*, 676–682. [CrossRef]
54. Puch, F.; Hopmann, C. Experimental investigation of the influence of the compounding process and the composite composition on the mechanical properties of a short-flax fiber reinforced polypropylene composite. *Polym. Compos.* **2015**, *36*, 2282–2290. [CrossRef]
55. Hoy, K.L. Solubility parameter as a design parameter for water borne polymers and coatings. *J. Paint Technol.* **1970**, *42*, 115–118. [CrossRef]
56. Bakhtiarian, E.; Foot, P.J.S.; Miller Tate, P.C. Conductive poly(epichlorohydrin)-polyaniline dodecylbenzenessulfonate in solution. *Progr. Rubber Plast Recycl. Technol.* **2016**, *32*, 183–200. [CrossRef]
57. Fried, J.R. *Polymer Science and Technology*, 3rd ed.; Prentice Hall: New York, NY, USA, 2014; pp. 101–152.
58. Kraus, G. Degree of cure in filler-reinforced vulcanizates by the swelling method. *Rubber Chem. Technol.* **1957**, *30*, 928–951. [CrossRef]
59. Kraus, G. Swelling of filler-reinforced vulcanizates. *J. Appl. Polym. Sci.* **1963**, *7*, 861–871. [CrossRef]
60. Mathew, L.; Joseph, K.U.; Joseph, R. Swelling behaviour of isora/natural rubber composites in oils used in automobiles. *Bull. Mater. Sci.* **2006**, *29*, 91–99. [CrossRef]
61. Parks, C.; Lorenz, O. Crosslinking efficiency in the reaction of dicumyl peroxide with dimethyloctadiene. *J. Polym. Sci.* **1961**, *50*, 287–298. [CrossRef]
62. Jacob, M.; Thomas, S.; Varughese, K.T. Mechanical properties of sisal/oil palm hybrid fiber reinforced natural rubber composites. *Comp. Sci. Technol.* **2004**, *64*, 955–965. [CrossRef]
63. Das, A.; Stockel Huber, K.W.; Wang, D.Y.; Galiatstos, V.; Heinrich, G. Understanding the reinforcing behavior of expanded clay partides in natural rubber compounds. *Soft Matter* **2013**, *9*, 3798–3808.
64. Pejića, B.M.; Kramara, A.D.; Obradovićb, B.M.; Kuraicab, M.M.; Žekićb, A.A.; Kostića, M.M. Effect of plasma treatment on chemical composition, structure and sorption properties of lignocellulosic hemp fibers (*Cannabis sativa* L.). *Carbohydr. Polym.* **2020**, *236*, 116000. [CrossRef]
65. Haghighatnia, T.; Abbasian, A.; Morshedian, J. Hemp fiber reinforced thermoplastic polyurethane composite: An investigation in mechanical properties. *Ind. Crops Prod.* **2017**, *108*, 853–863. [CrossRef]
66. Célino, A.; Gonçalves, O.; Jacquemin, F.; Fréour, S. Qualitative and quantitative assessment of water sorption in natural fibres using ATR-FTIR spectroscopy. *Carbohydr. Polym.* **2014**, *101*, 163–170. [CrossRef]
67. Lazorenko, G.; Kasprzhitskii, A.; Yavna, V.; Mischinenko, V.; Kukharskii, A.; Kruglikov, A.; Kolodina, A.; Yalovega, G. Effect of pre-treatment of flax tows on mechanical properties and microstructure of natural fiber reinforced geopolymer composites. *Env. Technol. Innov.* **2020**, *20*, 101105. [CrossRef]
68. Abidi, N.; Cabrales, L.; Haigler, C.H. Changes in the cell wall and cellulose content of developing cotton fibers investigated by FTIR spectroscopy. *Carbohydr. Polym.* **2014**, *100*, 9–16. [CrossRef]
69. Gunasekaram, S.; Natarajan, R.K.; Kala, A. FTIR spectra and mechanical strength analysis of some selected rubber derivatives. *Spectrochim. Acta Part A* **2007**, *68*, 323–330. [CrossRef] [PubMed]
70. Litvinov, V.M.; De, P.P. *Spectroscopy of Rubber and Rubbery Materials*; RAPRA Technol. Ltd.: Shawbury, UK, 2002.
71. Sing, K.S.W.; Everett, D.H.; Haul, R.A.W.; Moscou, L.; Pierotti, R.A.; Rouquerol, J.; Siemieniewska, T. Reporting physisorption data for gas/solid systems—With special reference to the determination of surface area and porosity. *Pure Appl. Chem.* **1985**, *57*, 603–619. [CrossRef]
72. Dhakal, H.N.; Zhang, Z.Y.; Richardson, M.O.W. Effect of water absorption on the mechanical properties of hemp fibre reinforced un saturated polyester composites. *Compos. Sci. Technol.* **2007**, *67*, 1674–1683. [CrossRef]
73. Brunauer, S.; Deming, L.S.; Deming, W.E.; Teller, E. On a theory of the van der Waals adsorption of gases. *J. Am. Chem. Soc.* **1940**, *62*, 1723–1732. [CrossRef]
74. Murray, K.L.; Seaton, N.A.; Day, M.A. An adsorption-based method for the characterization of pore networks containing both mesopores and macropores. *Langmuir* **1999**, *15*, 6728–6737. [CrossRef]